



# Shared universality of charged black holes and the complex large- $q$ Sachdev-Ye-Kitaev model

Jan C. Louw  and Stefan Kehrein

*Institute for Theoretical Physics, Georg-August-Universität Göttingen, Friedrich-Hund-Platz 1, 37077 Göttingen, Germany*

 (Received 20 June 2022; revised 31 January 2023; accepted 31 January 2023; published 13 February 2023)

We investigate the charged  $q/2$ -body interacting Sachdev-Ye-Kitaev (SYK) model in the grand-canonical ensemble. By treating  $q$  as a large parameter, we are able to analytically study its phase diagram. By varying the chemical potential or temperature, we find that the system undergoes a phase transition between low and high entropies in the maximally chaotic regime. A similar transition in entropy is seen in charged anti-de Sitter (AdS) black holes transitioning between a large and small event horizon. Approaching zero temperature, we find a first-order chaotic-to-nonchaotic quantum phase transition, where the finite extensive entropy drops to zero. This again has a gravitational analog—the Hawking-Page transition between a large black hole and thermal radiation. An analytical study of the critical phenomena associated with the continuous phase transition provides us with mean-field van der Waals critical and effective exponents. We find that all analogous power laws are shared with several charged AdS black hole phase transitions. Together, these findings indicate a connection between the charged  $q \rightarrow \infty$  SYK model and black holes.

DOI: [10.1103/PhysRevB.107.075132](https://doi.org/10.1103/PhysRevB.107.075132)

## I. INTRODUCTION

The analysis of condensed-matter systems lacking quasi-particles is hindered by the unamenability of Fermi-liquid theory. One successful approach is via a class of disordered Sachdev-Ye-Kitaev (SYK) models [1,2] or their related disorderless planar/tensor matrix models [3,4]. Despite their nonintegrability, one may find exact relations between the self-energy and Green's function  $\mathcal{G}$  [5]. This reduces the exponential complexity of the problem to a single Dyson equation purely in terms of  $\mathcal{G}$ . Although some analytical results exist in the infrared limit [6], the full solutions are obtained numerically.

There is also a framework in which one may find exact analytical solutions. This is by considering  $q/2$ -body interactions, for large  $q$ , and treating  $1/q$  as an expansion parameter. In this work we present a study of such a model [2,7],

$$\mathcal{H} = J \sum_{\substack{1 \leq i_1 < \dots < i_{q/2} \leq N \\ 1 \leq j_1 < \dots < j_{q/2} \leq N}} X_{j_1 \dots j_{q/2}}^{i_1 \dots i_{q/2}} c_{i_1}^\dagger \dots c_{i_{q/2}}^\dagger c_{j_{q/2}} \dots c_{j_1}, \quad (1)$$

with a conserved U(1) charge density  $\hat{Q} = \frac{1}{N} \sum_i c_i^\dagger c_i - 1/2$ , with expectation values  $Q \in [-1/2, 1/2]$ . Here  $c^\dagger, c$  are Dirac/complex fermionic creation and annihilation operators, respectively. We will study this model in the grand-canonical ensemble with partition function  $Z = \text{Tr}\{e^{-\beta[\mathcal{H} - \mu N \hat{Q}]}\}$ . The couplings,  $X$ , are complex random variables with zero mean and a variance  $|X|^2 = [q^{-1}(q/2)!]^2 [2/N]^{q-1}$ . Such models have the advantage of being amenable to analytical solutions. At neutral charge,  $Q = 0$ , its thermodynamics reduces to its Majorana ( $c^\dagger = c$ ) counterpart [6]. The inclusion of nonzero charge brings Eq. (1) in closer contact with electronic systems [1,8,9]. By varying a chemical potential  $\mu$ , the conjugate to  $Q$ , we find that this model exhibits a phase transition similar

to its finite- $q$  equivalents [3,10]. In contrast to the numerical results in the finite- $q$  case, we are able to analytically study its phase diagram in the large- $q$  limit. This is done by considering suitable polynomial scaling (in  $q$ ) thermodynamic variables such as  $T, \mu$ . Such  $q$  scalings have also previously been considered for two coupled Majorana SYK models [11] in the  $q \rightarrow \infty$  limit. The analytical solutions to the equilibrium Green's functions  $\mathcal{G}$  and a proof that they remain valid for our considered scaling is given in Appendix A.

The Green's functions are key to studying the phase diagram. This is because the Kubo-Martin-Schwinger (KMS) relation,  $\mathcal{G}(\tau + \beta) = -e^{-\beta\mu}\mathcal{G}(\tau)$  [12, Appendix B], allows one to extract the exact equation of state [7, Eq. (43)],

$$\mu(Q) = 2T \tanh^{-1}(2Q) + 4Q\mathcal{J}(Q) \sin(\pi v/2)/q, \quad (2)$$

for large  $q$  with effective coupling strength

$$\mathcal{J}(Q) \equiv J[1 - 4Q^2]^{(q-2)/4} \quad (3)$$

and the Lyapunov exponent  $\lambda_L = 2\pi vT$ , found by solving  $\mathcal{J}/T = \pi v \sec(\pi v/2)$  [6]. Note that for any nonzero  $Q = \mathcal{O}(q^0)$ , the interaction is suppressed for large  $q$ ,  $\mathcal{J} \xrightarrow{q \rightarrow \infty} 0$ .

One is able to retain nonzero (constant) effective coupling  $\mathcal{J}$  by adjusting the model to have  $Q$ -dependent coupling  $J(Q) \propto [1 - 4Q^2]^{(2-q)/4}$  [13]. This allows the interactions to remain relevant at all charge densities. Notice, however, that with this adjustment the Hamiltonian inherits a temperature dependence from the charge density [8]. In this case there is no phase transition. In contrast, by a suitable  $q$ -dependent rescaling introduced below, we will find that the phase transition of the Hamiltonian (1), without adjustments, persists even for  $q \rightarrow \infty$ .

In particular, we find a van der Waals (vdW)-like phase diagram [14,15], with a line of first-order phase transition

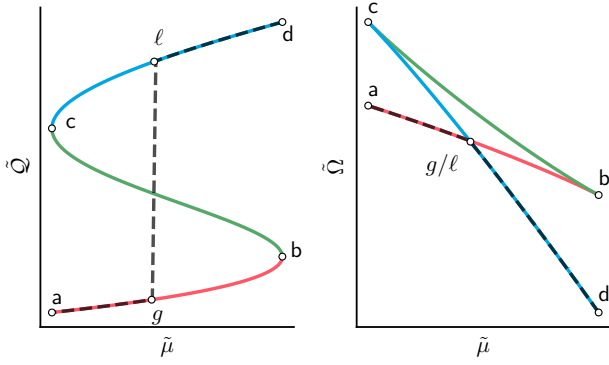


FIG. 1. The three solutions to Eq. (5) distinguished by color for  $\tilde{T} < \tilde{T}_{\text{crit}}$ . The dashed line indicates the thermodynamically favorable solution.

terminating at a critical end point where the transition is continuous. Associated with this are multiple power laws, the critical exponents of which we are able to calculate analytically. Comparing exponents, we find that our model shares such a universality class with a wide range of models, including numerous AdS black holes, a nonexhaustive list of which is in Refs. [15–22]. These similarities between black holes and the complex large- $q$  SYK model extend even beyond the shared universality class. For instance, over the phase transition there is a drop in entropy reminiscent of the large-to-small horizon transition in Reissner-Nordström (RN), charged and nonrotating, black holes. Such systems also appear in the study of non-Fermi liquids under the name RN metals [23].

*Phase diagram.* We start our analysis by considering two extremes. At zero charge density we are left with a strongly interacting pure Majorana-like SYK model, while at any finite charge density  $Q = O(q^0)$  the interaction (3) is trivial,  $\mathcal{J} \rightarrow 0$ , leaving a Fermi gas. Somewhere in between these two extremes must lie a regime where interactions and density terms in (2) compete in a nontrivial way. Indeed, such a competition is found for thermodynamic quantities which scale like

$$T = \tilde{T} q^{-1}, \quad \mu = \tilde{\mu} q^{-3/2}, \quad (4)$$

where tilde'd quantities are held fixed as  $q \rightarrow \infty$ . In turn, the charge densities scales like  $Q = \tilde{Q} q^{-1/2}$ , hence yielding a finite effective interaction (3),  $\mathcal{J}(Q) \xrightarrow{q \rightarrow \infty} e^{-\tilde{Q}^2} J$ . This scaling corresponds to the maximally chaotic regime where  $v = 1 - 2\tilde{T}/(q\mathcal{J}) + O(1/q^2)$  saturates the universal (chaos) bound  $\lambda_L \rightarrow 2\pi T$  [24]. Using the scaling (4) thus simplifies equation of state (2) to

$$\tilde{\mu}(\tilde{Q}) = 4\tilde{Q}[\tilde{T} + J e^{-\tilde{Q}^2}] + O(1/q). \quad (5)$$

Plotting this, as in Fig. 1, one notes that there exists a critical temperature,  $\tilde{T}_{\text{crit}} = 2J e^{-3/2}$ , below which three solutions exist instead of one. The solution from point b-c has unphysical negative compressibility. Such behavior is also seen in the vdW liquid-gas transition. Due to the difference in (charge) density and similarities to the vdW system, we shall refer to the two physical solutions as the gaseous and liquid phases, given in pink and blue, respectively.

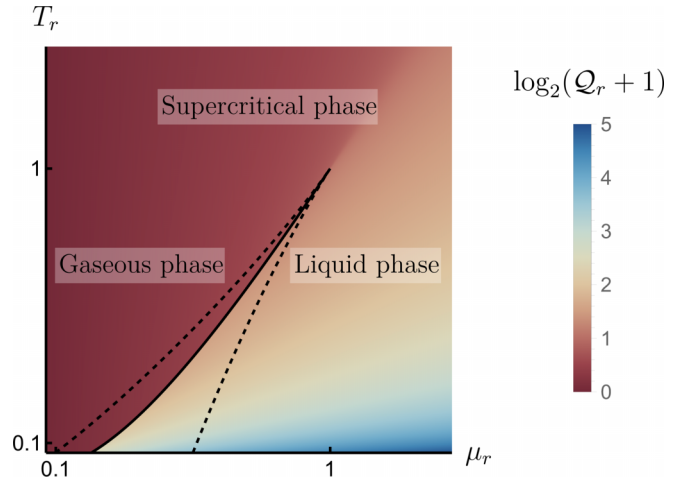


FIG. 2. Phase diagram, for scaling (4), in terms of reduced variables  $T_r = \tilde{T}/\tilde{T}_{\text{crit}}$ ,  $\mu_r = \tilde{\mu}/\tilde{\mu}_{\text{crit}}$ , and  $Q_r = \tilde{Q}/\tilde{Q}_{\text{crit}}$ . The solid and dashed lines denote the coexistence and stability curves, respectively. The color corresponds to the thermodynamically favorable charge density.

Out of the three, the thermodynamically favorable solution corresponds to the smallest grand potential (per lattice site)  $\Omega = -T \ln Z/N$ . Considering the partition function, we observe the relations  $J \partial_J \Omega = E$  and  $\partial_\mu \Omega = -Q$ , where the energy density is given by [7]

$$E = -2(1 - 4Q^2)\mathcal{J} \sin(\pi v/2)/q^2,$$

which defines a set of differential equations. From the relation  $\Omega = E - \mu Q - T\mathcal{S}$ , we observe that the entropy density  $\mathcal{S}$  is the only unknown. We may find  $\mathcal{S}$  by solving the set of differential equations for the scaling (4), i.e., in the maximal chaotic regime  $v \rightarrow 1$ ,  $\partial_\mu q^2 \Omega = -\tilde{Q}$  and  $\partial_J q^2 \Omega = -2e^{-\tilde{Q}^2}$ . One may then verify by substitution that  $\mathcal{S} = \ln 2 - 2\tilde{Q}^2/q + O(1/q^2)$ , where the constant is found by using the free fermion solution at  $J = 0$ . The corresponding grand potential is written as  $q^2 \Omega = \tilde{\Omega} - q\tilde{T} \ln 2$ , with

$$\tilde{\Omega} \equiv -2\tilde{Q}^2 \tilde{T} - 2[1 + 2\tilde{Q}^2]J e^{-\tilde{Q}^2} + O(1/q). \quad (6)$$

Considering  $\tilde{\Omega}$  for these three solutions, plotted in Fig. 1, we find that the favorable charge density necessarily jumps between  $g$  and  $\ell$ , missing the unphysical solution. Also note the distinct swallowtail shape, from catastrophe theory, which is also common to RN phase transitions. This shape is indicative of a first-order phase transition, in this case from a low (charge) density gaseous phase to the dense liquid phase. This is induced either by increasing the chemical potential or decreasing the temperature, as seen from the phase diagram in Fig. 2. The stability limit curves, enclosing the region where both phases can coexist, coincide at the critical point  $(\tilde{\mu}_{\text{crit}}, \tilde{T}_{\text{crit}})$ , with charge density  $\tilde{Q}_{\text{crit}} = \sqrt{3/2}$ . Here the two turning points b and c merge into an inflection point, where there is a continuous (second-order) phase transition. Above this lies the supercritical phase, identified by a single unique solution.

*Universality.* Approaching the critical point, i.e., for small shifted variables  $m \equiv \mu_r - 1$ ,  $\rho \equiv Q_r - 1$ , and  $t \equiv T_r - 1$ , we find that various thermodynamic quantities display power

TABLE I. Table of critical exponents.

$\alpha$	$\beta$	$\gamma$	$\delta$
0	1/2	1	3

laws. To study this we shift and rescale the grand potential (6) and consider it close to this point,

$$f = \frac{\tilde{\Omega} - \tilde{\Omega}_{\text{crit}}}{\tilde{\mu}_{\text{crit}} \tilde{Q}_{\text{crit}}} + t/3 + m = -\rho^2 \frac{t + (3\rho/2)^2}{3} + \mathcal{O}(\rho^5), \quad (7)$$

which satisfies  $\partial_m f = -\rho$ , stemming from  $\partial_{\tilde{\mu}} \tilde{\Omega} = -\tilde{Q}$ . Further, the linear shift  $t$  will not affect the specific heat.

In particular, we focus on the minimized grand potential corresponding to the dashed line in Fig. 1. One may show that in terms of some ordering field  $\tilde{\mathcal{H}}$ , it is homogeneous  $f(t, \tilde{\mathcal{H}}) = t^{2-\alpha} f(1, \tilde{\mathcal{H}} t^{\beta-2+\alpha})$ , where  $\alpha$  and  $\beta$  are the critical exponents characterizing the power laws. Models which share the same scale-invariant form  $f$  under the renormalization group flow are said to belong to the same universality class.

The homogeneity property is satisfied for the ordering field  $\tilde{\mathcal{H}} = m - 2t/3$ , which restricts the form of  $\tilde{\mathcal{H}}$  up to a scaling constant. This leaves the singular function

$$f(t, \tilde{\mathcal{H}}) = -\frac{|t|^{2-\alpha}}{6} - |\tilde{\mathcal{H}}| |2t/3|^\beta - \frac{3\tilde{\mathcal{H}}^2}{2} |t|^{-\gamma} + \mathcal{O}(\tilde{\mathcal{H}}^3 |t|^{-5/2})$$

for small  $\tilde{\mathcal{H}}$  and  $f(t, \tilde{\mathcal{H}}) = -\frac{3}{4} |\tilde{\mathcal{H}}|^{1+1/\delta} [1 + \mathcal{O}(t \tilde{\mathcal{H}}^{-2/3})]$  for small  $t$ . The details of this calculation are given in Appendix C. Here  $\alpha$ ,  $\beta$ ,  $\gamma$ ,  $\delta$  are the classical mean-field critical exponents, given in Table I. As such, our model falls into the vdW universality class. From  $\rho(t, \tilde{\mathcal{H}}) = -\partial_{\tilde{\mathcal{H}}} f(t, \tilde{\mathcal{H}})$ , we have  $\rho(0, \tilde{\mathcal{H}}) = \tilde{\mathcal{H}}^{1/\delta}$ , and

$$\rho(t, \tilde{\mathcal{H}}) = \text{sgn}(\tilde{\mathcal{H}}) |2t/3|^{1/2} + 2\tilde{\mathcal{H}} |2t/3|^{-1} + \mathcal{O}(\tilde{\mathcal{H}}^2 t^{-5/2}) \quad (8)$$

for small  $\tilde{\mathcal{H}}$ . The remaining critical exponents characterize the power laws along the line  $\tilde{\mathcal{H}} = 0$ : the order parameter  $\rho(t, 0) \propto |t|^\beta$ , specific heat  $C_{\tilde{\mathcal{H}}} \propto -\partial_t^2 f(t, 0) \propto |t|^{-\alpha}$ , and susceptibility  $\chi_{\tilde{\mathcal{H}}} \propto \partial_{\tilde{\mathcal{H}}}^2 f(t, \tilde{\mathcal{H}})|_{\tilde{\mathcal{H}}=0} \propto |t|^{-\gamma}$ .

*Effective exponents.* The particular power law can be dependent on the line along which the critical point is reached. This feature is due to the mixing of chemical potential and temperature in the ordering field  $\tilde{\mathcal{H}}$  [25]. Since the corresponding exponents do not enter into the scale-invariant form of the model, they are not the critical exponents which define the universality class. However, these *effective* exponents still describe physically relevant processes. As an example, let us consider the specific heat. For constant  $\mu$ , we have  $C_\mu \propto -\partial_t^2 f(t, -2t/3) \propto |t|^{-2/3}$ , i.e.,  $\alpha_\mu = 2/3$ . Here, the subscripts indicate which quantity is set to its critical value. In contrast, for constant  $Q$ , we use the identity  $C_Q = (\partial_T E)_Q$ . In the chaotic regime, the energy behaves as  $E \propto T^2 + \text{const.}$ , leaving  $C_Q \propto T \sim t^0$ . While often associated with Fermi-liquid behavior, such as a Sommerfeld, linear in  $T$ , specific heat also appears in RN [23] and cuprate [26–28] strange metals for a range of doping levels. The remaining *effective* exponents can be obtained from (8) and are listed in Tables II(a) and II(b).

*Relation to gravity.* By comparing order parameters and their conjugates, one can make various analogies between

TABLE II. Tables of effective exponents.

(a)	$\alpha_\mu$	$\beta_\mu$	$\gamma_\mu$
	2/3	1/3	2/3
(b)	$\alpha_Q$	$\gamma_Q$	
	0	1	

the models listed in Table III. The similarities are strongest when comparing our model to RN black holes. These systems are defined by a charge  $q_B$ , an event horizon radius  $r$ , and electrical potential  $\Phi = q_B r^{2-d}$  [22]. One may also consider such systems in an *extended* AdS $_{d+1}$  space [15,29], where the cosmological constant  $\Lambda$  and its conjugate quantity, the volume  $V$ , are treated as thermodynamic variables. Here  $V$ , like in the vdW case, is the order parameter, while  $-\Lambda$  acts as the pressure term  $P$ .

These analogies are quantitative in the sense that all effective exponents also match. By this we mean that by keeping order parameters fixed, both exponents match II(b). Then, while keeping the conjugates fixed, we find three exponents matching II(a). All models listed in Table III also share the same critical exponents. As such, our model, the vdW liquid [15], and multiple RN AdS $_{d+1}$  black holes [15,17,22,29] all share a universality class, as well as having the same effective exponents.

Besides sharing a universality class, these analogous models also have an abundance of qualitative commonalities. This is particularly apparent at low energies where the suppression by large charge densities leaves a relatively weakly interacting,  $\mathcal{J} \sim e^{-Q^2} J$ , liquid phase. The extreme of this is seen by considering a different rescaling,

$$T = \bar{T} q^{-2}, \quad \mu = \bar{\mu} q^{-2}, \quad (9)$$

where the system transitions to a finite nonrescaled charge density  $Q = 0 \rightarrow \sqrt{1 - e^{-4J/\bar{T}}}/2$ , shown in Appendix B. This suppresses the effective interaction  $\mathcal{J} = e^{-qJ/T} J \rightarrow 0$ , yielding a free integrable ( $v \rightarrow 0$ ) system. As such, small perturbations, stemming from  $\bar{\mu}$  to the  $Q = 0$  symmetric-Majorana state, induce a jump to a Fermi gas at finite (positive or negative) charge density, hence breaking the U(1) symmetry. This transition is thus from a maximally chaotic to a nonchaotic state. Such a Fermi gas has an entropy  $S = -\beta\mu Q - \ln \sqrt{1/4 - Q^2}$ . To leading order in  $\bar{T} \equiv \bar{\beta}^{-1}$ , this indicates a drastic drop in entropy,  $\ln 2 \rightarrow \bar{\beta} J e^{-4\bar{\beta} J}$ . Such an instability is also seen in RN black holes at low temperatures [30,31]. The RN transition is from a large black hole to a small one. Since the Bekenstein-Hawking entropy is proportional to the surface area, this also corresponds to a drop in entropy.

TABLE III. Analogies between models with shared universality class.

Model	SYK	vdW	RN-AdS	
	[7]	[14,15]	[15,29]	[17]
Order parameter	$Q$	$V$	$V$	$\Phi$
Conjugate	$\mu$	$P$	$-\Lambda$	$q_B$

Lastly, both RN and SYK transitions also include an unstable solution with a negative bulk modulus.

For  $\bar{T} = o(q^0)$ , there is a first-order quantum phase transition from  $\mathcal{Q} = 0$  to maximum density  $\mathcal{Q} = 1/2$  at  $\bar{\mu}_0 = 4J$ . If  $\bar{\mu} < \bar{\mu}_0$ , then we are left with a Majorana SYK ground-state solution with an extensive entropy. Such a finite entropy, at  $T = 0$ , is also the defining property of RN metals [23]. If  $\bar{\mu} > \bar{\mu}_0$ , we are left with a zero-entropy harmonic oscillator vacuum state. This first-order quantum phase transition is also observed in the finite- $q$  equivalent models [3,10]. Such a transition is again related to gravity, this time the classical HP transition [32], which has a large black hole to (noninteracting) thermal radiation with a zero entropy transition.

Also of note is the conjecture of black holes being the fastest scramblers [33] and as such chaotic [6,34,35]. Assuming this holds, the gravitational analogies extend over to a chaotic-to-chaotic RN transition, as we found in the scaling regime (4). It would further include a chaotic-to-nonchaotic HP transition, where the nonchaotic phase is (noninteracting) thermal radiation, corresponding to our observed low-temperature crossover (9).

It is quite remarkable that there are at least two RN models which also qualitatively match our phase diagram [17,21] by terminating at a first-order phase transition at  $(q_B, \beta) = (0, \beta_Z)$ . This is reminiscent of how our coexistence line terminates at  $(\bar{T}, \bar{\mu}) = (0, \bar{\mu}_0)$ . This is in contrast to extended-space RN black holes and vdW, with coexistence lines extending to the point (0,0). At the other end, both models terminate at a second-order transition. Of note is that [21] has the same effective exponents matching II(a) [22].

All these similarities are perhaps not so surprising from the perspective of holography. This is because the SYK model is a  $(0+1)$ -dimensional conformally symmetric theory at low temperatures. As such, from the anti-de Sitter/conformal field theory (AdS/CFT) correspondence, one would conjecture that it is a CFT on the boundary of some  $\text{AdS}_{1+1}$  space. Standard  $(1+1)$ -dimensional gravity is topological and displays only trivial physics; hence we consider nonstandard gravity, the simplest of which are the Jackiw-Teitelboim (JT) black holes. They may be viewed as the dimensional reduction, or the near-horizon theory of near-extremal (minimal mass) higher-dimensional black holes [36–38]. One such model [18] even has a phase transition with calculated effective exponents matching that of II(b) and  $\beta = 1/2$ .

## II. CONCLUSION

We presented an analytic study of the complex large- $q$  SYK model, showing that it displays an RN-like phase transition. Prior numerical analyses of the finite- $q$  case have observed that the phase diagram scales away at larger values of  $q$  [3,10]. We showed that if one considers rescaled quantities as described by (4) and (9), then the transition in fact still exists at infinite  $q$ .

One can further study the overlap of our large- $q$  results with that of the finite- $q$  numerical results [10]. A natural choice is to consider the relative error between their respective critical values. Such an analysis is provided in Appendix D, where we found relative errors which appear to converge to

zero rather quickly as  $q$  increases. This supports the relevance of the  $q \rightarrow \infty$  limit for finite- $q$  models.

In contrast to the finite- $q$  case, which has asymmetric (differing over the coexistence line) irrational exponents [3,10], we found symmetric rational numbers. One should note that Refs. [3,10] actually determined effective exponents because the ordering field was assumed to be the chemical potential. However, as we have seen in our analysis, field mixing needs to be taken into account to determine the universality class and the critical exponents. The only exception where field mixing plays no role is  $\beta$ . The small deviation from the mean-field value  $1/2$  in Refs. [3,10] might be due to numerical error, and as such whether the finite- $q$  SYK model also falls into the vdW universality class remains an open question.

By comparing the critical exponents to other models, we found that the complex large- $q$  SYK model and many RN black holes find themselves in the same mean-field vdW universality class. Further, in the low-reduced-temperature regime, defined by the scaling (9), we found a jump between maximally chaotic and nonchaotic phases, also observed in generalized/coupled SYK models [11,39–43]. The coexistence line dividing the two phases terminates at a first-order quantum phase transition from a Majorana ground state to a Fermi gas, and hence a drop from nonzero residual entropy down to zero. This feature is shared with the first-order Hawking-Page (HP) transition between a large black hole and thermal radiation [32]. As such, the gravitational analogies extend to the low-temperature regime.

From the perspective of AdS/CFT, these similarities between our model and charged black holes are perhaps not too surprising. This is because the SYK model is conformally symmetric in the infrared limit [6]. However, the details narrow down the list of possible gravity duals to the SYK model [44]. The analytical expressions derived in this work, the power laws, equation of state, and grand potential serve as a guide towards finding this dual.

We conclude with the natural question of whether any columns in Table III or other mentioned analogies are part of an AdS/CFT dictionary. In other words, is there (asymptotic) equivalence between any of the partition functions?

## ACKNOWLEDGMENTS

We would like to thank Peter Sollich for helpful discussions on field mixing, critical exponents, and scaling relations. This work was funded by the Deutsche Forschungsgemeinschaft (DFG, German Research Foundation) - 217133147/SFB 1073, Project B03, and the Deutsche akademische Austauschdienst (DAAD, German Academic Exchange Service).

## APPENDIX A: VALIDITY OF $q$ RESCALING

The thermal Green's function  $\mathcal{G}(\tau - \tau') \equiv \mathcal{G}(\tau, \tau') = -\mathcal{T}\langle c(\tau)c^\dagger(\tau') \rangle$  is the solution to Dyson's equation:

$$[\mathcal{G} - \mathcal{G}_0](\tau, \tau') = \int_0^\beta d\tau_1 dt \mathcal{G}(\tau, t) \Sigma(t, \tau_1) \mathcal{G}_0(\tau_1, \tau'), \quad (\text{A1})$$



with noninteracting Green's function  $\mathcal{G}_0(\tau) = \langle c^\dagger c \rangle_0 - \Theta(\tau)$  and self-energy  $\Sigma$ . For the  $q/2$ -body interacting SYK model,  $\Sigma(t) = \mathcal{G}(t)2J^2[-4\mathcal{G}(t)\mathcal{G}(-t)]^{q/2-1}/q$  [2]. We write  $\mathcal{G}(\tau) = [Q - \text{sgn}(\tau)/2]e^{\Delta\mathcal{G}(\tau)}$ , with  $\Delta \equiv 1/q$ , leaving  $q\Sigma = 2\mathcal{J}^2 e^{(1-2\Delta)\mathcal{G}_+} \mathcal{G}$ . Here we have it split into symmetric/asymmetric parts  $\mathcal{g}_\pm(-\tau) = \pm\mathcal{g}_\pm(\tau)$  and defined the charge density  $\mathcal{Q} \equiv \frac{1}{N} \sum_i \langle c_i^\dagger c_i \rangle - 1/2$ .

*Claim 1.* In the large- $q$  limit, we *claim* that for any thermodynamic variables which scale subexponentially in  $q$ , the solution to (A1) is given by  $\mathcal{g}_-(\tau) = 2\mathcal{Q}\mathcal{g}_+(0)\tau$  and

$$e^{[1-2\Delta]\mathcal{g}_+(\tau)} = \frac{[\pi v/\lambda]^2}{\cos^2[\pi v(1/2 - |\tau|/\beta)]}, \quad \frac{\pi v/\lambda}{\cos[\pi v/2]} = 1, \quad (\text{A2})$$

where  $\lambda = \beta\mathcal{J}\sqrt{1-2\Delta}$  and  $\mathcal{J} \equiv [1-4\mathcal{Q}^2]^{(q-2)/4}J$ . Note that for nonrescaled variables, they take on the standard known forms given for neutral charge  $\mathcal{Q} = 0$  in [6] or at finite charge in [7].

*Proof.* We take the approach of substituting the claimed solutions  $\mathcal{g}_\pm$  into the full Dyson equation. We then gather the nonzero (error) terms  $\Delta R_i$  and show that, given sub-exponentially scaling,  $\Delta R_i \xrightarrow{\Delta \rightarrow 0} 0$ . Using (A1),  $q\partial_\tau \ln \mathcal{G}(\tau, \tau')|_{\tau'=0}$ , for  $\tau \geq 0$ , reduces to

$$\dot{\mathcal{g}}(\tau) - \mathcal{J}^2 \int_0^\beta dt [\text{sgn}(\tau - t) - 2\mathcal{Q}] e^{\mathcal{g}_+(\tau) + \Delta\varphi_\tau(t)} = 0, \quad (\text{A3})$$

with  $\varphi_\tau(t) \equiv \mathcal{g}(\tau - t) - \mathcal{g}(\tau) - \mathcal{g}(-t)$ . By differentiating again we obtain the two equations

$$\ddot{\mathcal{g}}_+ = 2\mathcal{J}^2 e^{[1-2\Delta]\mathcal{g}_+} [1 + \Delta R], \quad \ddot{\mathcal{g}}_- = \Delta 2\mathcal{Q}\mathcal{J}^2 R_3,$$

with  $R \equiv R_1 + R_2$ . Ignoring the error terms, we have  $\mathcal{g}_-(\tau) \sim \epsilon\tau$ , while  $\ddot{\mathcal{g}}_+$  reduces to a Liouville equation with solution (A2). The boundary condition in (A2) enforces  $\mathcal{G}(0^+) = \mathcal{Q} - 1/2$ . By substituting the solutions back into (A3), one finds the error terms

$$R_1(\tau) = -[e^{-(1/2-\Delta)\mathcal{g}_+(\tau)} \dot{\mathcal{g}}_+(\tau)/\mathcal{J}]^2/2, \quad (\text{A4})$$

$$R_2(\tau) = e^{-(1+\Delta)\mathcal{g}_+(\tau)} \frac{\mathcal{I}_\tau(t)|_0^\tau - \mathcal{I}_{\tau+\beta}(t)|_\tau^\beta}{2}, \quad (\text{A5})$$

$$R_3(\tau) = -[\mathcal{I}_\tau(t)|_0^\tau + \mathcal{I}_{\tau+\beta}(t)|_\tau^\beta] - \frac{\dot{\mathcal{g}}_+(\tau) \dot{\mathcal{g}}_-(\tau)}{\mathcal{J} 2\mathcal{Q}\mathcal{J}}, \quad (\text{A6})$$

where we have defined the indefinite integral

$$\mathcal{I}_\tau(t) \equiv \int dt \dot{\mathcal{g}}_+(\tau - t) e^{\Delta\mathcal{g}_+(\tau-t) + (1-\Delta)\mathcal{g}_+(t)}. \quad (\text{A7})$$

We would next like to find the  $q$ -dependent scaling conditions on  $\lambda$  for which all  $\Delta R_i \xrightarrow{\Delta \rightarrow 0} 0$ . Using (A2), the bound  $|R_1| \lesssim 2$  follows from

$$\frac{\dot{\mathcal{g}}_+(\tau)}{\mathcal{J}} = -\frac{2 \sin[\pi v(1/2 - \tau/\beta)]}{\sqrt{1-2\Delta}} e^{(1/2-\Delta)\mathcal{g}_+(\tau)}.$$

To bound (A5) and (A6), we first evaluate the integral (A7). To simplify the analysis we would like to replace exponentials like  $e^{(1+\Delta)\mathcal{g}_+}$  with  $e^{\mathcal{g}_+}$ , under the integral, which is justified if the corresponding function, e.g.,  $e^{\Delta\mathcal{g}_+}$ , remains differentiable under said limit. To see when this holds, we note that  $(\pi v/\lambda)^{2\Delta} \leq e^{\Delta(1-2\Delta)\mathcal{g}_+(t)} \leq 1$  saturates for  $|\ln[v/\lambda]| \lesssim q$ . In

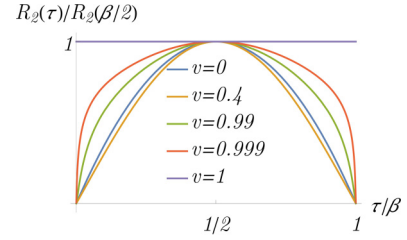


FIG. 3. The error plotted for various values of  $v$ .

this case, (A7) evaluates to

$$\begin{aligned} \mathcal{I}_\tau(t) &= \int dy \tan[\pi v/2 - (x-y)] \frac{-2 \cos^2(\pi v/2)}{\cos^2[\pi v/2 - y]} \\ &= 2 \cot[\pi v - x] \sin y \frac{\cos[\pi v/2]}{\cos[\pi v/2 - y]} \\ &\quad + 2 \left[ \frac{\cos(\pi v/2)}{\sin(\pi v - x)} \right]^2 \ln \frac{\cos[\pi v/2 - (x-y)]}{\cos(\pi v/2 - y)}, \quad (\text{A8}) \end{aligned}$$

where  $x = \pi v\tau/\beta$  and  $y = \pi vt/\beta$ . This yields the error (A5)

$$\begin{aligned} R_2(\tau) &\sim \left[ \frac{\csc^2[\pi v - x] + \csc^2 x}{2} \mathcal{g}_+(\tau) - 1 \right. \\ &\quad \left. + \frac{2 \sin^2[\pi v/2]}{\sin[\pi v - x] \sin x} \right] 2 \cos^2[\pi v/2 - x], \end{aligned}$$

which, seen in Fig. 3, has a maximum at  $\tau = \beta/2$  given by

$$R_2(\beta/2) = 2 + 2 \frac{\ln[\pi v/\lambda]^2}{1 - [\pi v/\lambda]^2}.$$

The final error term (A6) is bounded by using (A3) to write

$$\dot{\mathcal{g}}_-(\tau) \xrightarrow{\Delta \rightarrow 0} -2\mathcal{Q}\mathcal{J}^2 \int_0^\beta dt e^{\mathcal{g}_+(t)} = -\mathcal{Q} \int_0^\beta dt \ddot{\mathcal{g}}_+(t),$$

which integrates to  $\dot{\mathcal{g}}_-(\tau) = 2\mathcal{Q}\dot{\mathcal{g}}_+(0)$ , hence matching the postulated solution. Together with (A8), one may show that this leaves an error with maximum magnitude of  $4 \sin^2(\pi v/2)$  at  $\tau = 0$ .

With all three of these error terms, one notices that  $\Delta R_i \xrightarrow{q \rightarrow \infty} 0$  as long as large  $|\ln[v/\lambda]| \lesssim q$ . For large  $\lambda$ , the relation (A2) implies that  $v \sim 1$ . This means our solutions remains valid for any  $\ln \beta\mathcal{J} \ll q$ , which includes the polynomial scalings  $\beta\mathcal{J} \sim q^\alpha$  considered in the work, i.e.,  $T = \tilde{T}q^{-1}$  and  $T = \tilde{T}q^{-2}$ , with  $J = \mathcal{O}(q^0)$ . ■

## APPENDIX B: LOW-TEMPERATURE CHARGE TRANSITION

*Claim 2.* At small reduced temperature  $T_r \equiv \tilde{T}/\tilde{T}_{\text{crit}}$ , where  $\tilde{T}_{\text{crit}} = 2e^{-3/2}J$ , the charge density jumps as

$$\mathcal{Q}_g = \frac{\cosh^{-1}[e^{2\tilde{\beta}J}]}{q2\tilde{\beta}J} \rightarrow \mathcal{Q}_\ell = \frac{\sqrt{1 - e^{-4\tilde{\beta}J}}}{2}. \quad (\text{B1})$$

For convenience, we have defined  $\tilde{T} \equiv q^{-1}\bar{T}$ ,  $\tilde{\mu} \equiv q^{-1/2}\bar{\mu}$ .

As a special case, if we consider  $\tilde{T}$ ,  $\tilde{\mu}$  fixed in the large- $q$  limit, we find a transition from  $\mathcal{Q} = 0 \rightarrow \sqrt{1 - e^{-4\tilde{\beta}J}}/2$ , i.e.,

a transition to a finite nonrescaled charge density as discussed in the work.

*Proof.* Consider the grand and chemical potentials

$$\tilde{\Omega} = -2\mathcal{J} - 2\tilde{Q}^2[2\mathcal{J} + \tilde{T}], \quad \tilde{\mu} = 4\tilde{Q}[\mathcal{J} + \tilde{T}], \quad (\text{B2})$$

at low reduced temperature. In other words, consider the asymptotic behavior for  $\tilde{T} \ll J$  of the charge densities on both sides of the coexistence line. Though we do not have explicit forms for these charge densities, we can gain some insight by considering Fig. 1 from the work. Here we note that the gaseous solution must be smaller than the charge density at the first turning point of  $\tilde{\mu}(\tilde{Q})$ ,  $\tilde{Q}_g < \tilde{Q}_b$ , while the liquid charge density must be larger than the second turning point  $\tilde{Q}_\ell > \tilde{Q}_c$ . These turning points are

$$\tilde{Q}_b = \sqrt{\frac{1}{2} - w_0 \left[ \frac{-T_r}{e} \right]}, \quad \tilde{Q}_c = \sqrt{\frac{1}{2} - w_{-1} \left[ \frac{-T_r}{e} \right]}, \quad (\text{B3})$$

where  $w(x)$  is the product log satisfying  $w e^{wx} = x$ . Here the subscripts indicate the various branches, with  $w_0$  corresponding to the principal branch.

On the gaseous side we have  $\tilde{Q}_b = \sqrt{1/2} + \mathcal{O}(T_r)$ , implying relatively small charge densities  $\tilde{Q}_g < \sqrt{1/2}$ . As such, the strong coupling  $\mathcal{J}_g \equiv J e^{-\tilde{Q}_g^2} = \mathcal{O}(T_r^0)$  dominates in (B2),

$$\tilde{\Omega}_g = -2\mathcal{J}_g - 4\tilde{Q}_g^2[\mathcal{J}_g + \mathcal{O}(T_r)], \quad \tilde{\mu}_g = 4\tilde{Q}_g[\mathcal{J}_g + \mathcal{O}(T_r)]. \quad (\text{B4})$$

For the liquid phase we have  $\tilde{Q}_c = \sqrt{\ln[\beta_r \ln \beta_r]} + \mathcal{O}(1)$ , with  $\beta_r \equiv 1/T_r$ . As such, we have a relatively large charge density  $\tilde{Q}_\ell > \tilde{Q}_c$ , hence a large suppression in the coupling  $\mathcal{J}_\ell \lesssim \tilde{T} / \ln \beta_r$ . With this (B2) reduces to

$$\tilde{\Omega}_\ell = -2\tilde{T} \tilde{Q}_\ell^2 [1 + \mathcal{O}(\mathcal{J}_\ell/\tilde{T})], \quad \tilde{\mu}_\ell = 4\tilde{Q}_\ell \tilde{T} [1 + \mathcal{O}(\mathcal{J}_\ell/\tilde{T})], \quad (\text{B5})$$

where  $\mathcal{J}_\ell/\tilde{T} = \mathcal{O}(1/\ln \beta_r)$ . Here, the weakly interacting phase (B5) is in fact the leading-order solution to free fermions,

$$\tilde{\Omega}_0 = \frac{\tilde{T}}{2} \ln [1 - 4Q_\ell^2], \quad \tilde{\mu}_0 = 2 \frac{\tilde{T}}{\sqrt{q}} \tanh^{-1}[2Q_\ell], \quad (\text{B6})$$

i.e., expanding (B6) for small nonrescaled charge densities  $Q \equiv \tilde{Q}/\sqrt{q}$  yields (B5) to leading order. These are the full solutions at large charge densities, since this yields small effective interactions. An analysis using (B5), while valid at infinite  $q$ , for fixed tilde'd variables yields the incorrect zero-temperature limit expressions for large finite  $q$ . As such, we focus on phase transitions from (B4) to (B6), which includes the previous analysis as a solution under the appropriate limit. The phase transition occurs at the point of equal grand and chemical potential. Equating the expressions in (B4) and (B6) yields the equations

$$\ln(1 - 4Q_\ell^2) = -4\tilde{\beta} \mathcal{J}_g [1 + 2\tilde{Q}_g^2], \quad 2Q_\ell = \tanh[2\tilde{Q}_g \tilde{\beta} \mathcal{J}_g],$$

where  $\tilde{Q} \equiv q^{-1/2} \tilde{Q}$ . The solution to these two are the roots of

$$F(\tilde{Q}_g) = 1 + 2\tilde{Q}_g^2 - \frac{\ln \cosh[2\tilde{\beta} \mathcal{J}_g \tilde{Q}_g]}{2\tilde{\beta} \mathcal{J}_g}. \quad (\text{B7})$$

As  $\tilde{T} \rightarrow 0$ , the root is at  $\tilde{Q}_g = 1 + 2\tilde{Q}_g^2 \sim 1$ . Together with (B4), this suggests that there is a first-order transition at

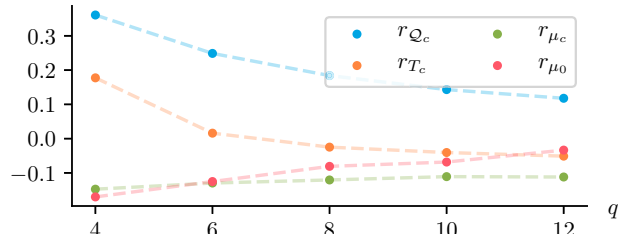


FIG. 4. Plots of the relative errors (D1) between the large- $q$  estimated critical points and the numerically calculated critical points for various finite  $q$  values.

$\tilde{\mu}_0 = 4J$ . Above zero temperature, for any  $\tilde{Q}_g = o(q^0)$  we simply have  $\mathcal{J}_g \sim J$  and as such the root of  $F$ ,  $\tilde{Q}_g$ , and the corresponding liquid charge density as given in (B1). ■

### APPENDIX C: SCALE-INVARIANT GRAND POTENTIAL

*Claim 3.* Consider the shifted rescaled grand potential from the work

$$f = -\rho^2[3\rho^2/4 + t/3] + \mathcal{O}(\rho^5). \quad (\text{C1})$$

Here  $\rho$  is the solution to the equation of state (B5) around the critical point

$$m - 2t/3 = \rho(2t/3 + \rho^2) + \mathcal{O}(\rho^4), \quad (\text{C2})$$

with  $m, t$ , and  $\rho$  defined in the work. We claim that in terms of the ordering field  $\tilde{h} = m - 2t/3$  that (C1) is homogeneous  $f(\tilde{h}, t) = t^2 f(1, \tilde{h}|t|^{-3/2})$ .

*Proof.* The above function  $f$  satisfies  $\partial_m f = -\rho$ . We may rewrite  $f$  in terms of  $\rho \equiv -|t|^{1/2} \Psi$ , as  $f = |t|^2 \Psi$ , where for  $t < 0$ ,

$$\Psi \equiv -\dot{\Psi}^2[3\dot{\Psi}^2/4 - 1/3] + \mathcal{O}(\rho^5).$$

To prove homogeneity, we must show that  $\dot{\Psi}$  is a function only of  $\omega \equiv \tilde{h}|t|^{-3/2}$ , hence leaving  $\Psi(\omega) \equiv f(1, \omega)$ . From (C2) we have the relation  $\omega = \dot{\Psi}(\Psi^2 - 2/3)$ . This implies that  $\dot{\Psi}$  is indeed purely a function of  $\omega$ . One may further show that  $\partial_\omega \Psi(\omega) = \dot{\Psi}(\omega)$ . The liquid phase solution is

$$\dot{\Psi}_\ell(\omega) = \begin{cases} [2/3]^{1/2} + 3\omega/4 - (3/2)^{7/2} \omega^2/4 + \mathcal{O}(\omega^3) \\ \omega^{1/3} + 2\omega^{-1/3}/9 + \mathcal{O}(\omega^{-5/3}). \end{cases}$$

Over the range  $\dot{\Psi} \leq 2^{3/2}/3$ ,  $\omega(\dot{\Psi})$  is three-to-one, with the two remaining solutions  $\dot{\Psi}_{b-c}(\omega) = \dot{\Psi}_\ell(-\omega) - \dot{\Psi}_\ell(\omega)$  and  $\dot{\Psi}_g(\omega) = -\dot{\Psi}_\ell(-\omega)$ , where the latter corresponds to the gaseous phase. Explicitly,

$$\Psi_\ell(\omega) = \begin{cases} -1/9 - \sqrt{2/3}\omega - 3\omega^2/8 + \mathcal{O}(\omega^3) \\ -\frac{3}{4}\omega^{4/3} - \frac{\omega^{2/3}}{3} - \frac{2}{27} + \mathcal{O}(\omega^{-2/3}). \end{cases}$$

Considering the grand potential, one notes that the gaseous solution is thermodynamically preferred for  $\omega < 0$  while the liquid solution is preferred for  $\omega > 0$ , i.e.,  $\dot{\Psi}^*(\omega) = \text{sgn}(\omega)\dot{\Psi}_\ell(|\omega|)$ . ■

### APPENDIX D: OVERLAP WITH FINITE- $q$ MODEL

We can test the extent to which our large- $q$  results capture the finite- $q$  physics by comparing our derived quantities to the

numerically derived ones in [10, Table I]. We focus on the relative error

$$r_x = \frac{x}{x^{(q)}} - 1, \quad (\text{D1})$$

where  $x$  is the large- $q$  estimation, while  $x^{(q)}$  corresponds to the numerical results. The particular quantities we compare are the critical values

$$\mathcal{Q}_c = \sqrt{\frac{3}{2q}}, \quad T_c = \frac{2Je^{-3/2}}{q}, \quad \mu_c = 6\mathcal{Q}_c T_c, \quad \mu_0 = \frac{4J}{q^2}$$

derived in the work. We choose a matching coupling constant to [10],  $J = \sqrt{q}2^{1-q}$ . As such, all the critical values become functions of  $q$ , which we compare with their numerically derived values in Fig. 4.

The comparison is given for  $q \in \{4, 6, 8, 10, 12\}$ . From this we note that the estimated values appear to converge to their finite  $q$  values rather fast as  $q$  increases. In order to reduce the relative error at smaller values of  $q$ , for instance,  $q = 4$ , one would have to consider  $1/q^2$  corrections to the Green's functions [45].

- 
- [1] S. Sachdev, Bekenstein-Hawking Entropy and Strange Metals, *Phys. Rev. X* **5**, 041025 (2015).
- [2] W. Fu, The Sachdev-Ye-Kitaev model and matter without quasiparticles, Ph.D. thesis, Harvard University, 2018.
- [3] T. Azeyanagi, F. Ferrari, and F. I. Schaposnik Massolo, Phase Diagram of Planar Matrix Quantum Mechanics, Tensor, and Sachdev-Ye-Kitaev Models, *Phys. Rev. Lett.* **120**, 061602 (2018).
- [4] E. Witten, An SYK-like model without disorder, [arXiv:1610.09758](https://arxiv.org/abs/1610.09758).
- [5] S. Sachdev and J. Ye, Gapless Spin-Fluid Ground State in a Random Quantum Heisenberg Magnet, *Phys. Rev. Lett.* **70**, 3339 (1993).
- [6] J. Maldacena and D. Stanford, Remarks on the Sachdev-Ye-Kitaev model, *Phys. Rev. D* **94**, 106002 (2016).
- [7] J. C. Louw and S. Kehrein, Thermalization of many many-body interacting Sachdev-Ye-Kitaev models, *Phys. Rev. B* **105**, 075117 (2022).
- [8] C. Zanoci and B. Swingle, Near-equilibrium approach to transport in complex Sachdev-Ye-Kitaev models, *Phys. Rev. B* **105**, 235131 (2022).
- [9] X. Y. Song, C. M. Jian, and L. Balents, Strongly Correlated Metal Built from Sachdev-Ye-Kitaev Models, *Phys. Rev. Lett.* **119**, 216601 (2017).
- [10] F. Ferrari and F. I. Schaposnik Massolo, Phases of melonic quantum mechanics, *Phys. Rev. D* **100**, 026007 (2019).
- [11] J. Maldacena and X. Qi, Eternal traversable wormhole, [arXiv:1804.00491](https://arxiv.org/abs/1804.00491).
- [12] N. Sorokhaibam, Phase transition and chaos in charged SYK model, *J. High Energy Phys.* **07** (2020) 055.
- [13] R. A. Davison, W. Fu, A. Georges, Y. Gu, K. Jensen, and S. Sachdev, Thermoelectric transport in disordered metals without quasiparticles: The Sachdev-Ye-Kitaev models and holography, *Phys. Rev. B* **95**, 155131 (2017).
- [14] W. Cho, D. Kim, and J. Park, Isobaric critical exponents: Test of analyticity against NIST reference data, *Front. Phys.* **6**, 00112 (2018).
- [15] D. Kubizňák and R. B. Mann, P-V criticality of charged AdS black holes, *J. High Energy Phys.* **07** (2012) 033.
- [16] B. R. Majhi and S. Samanta, P-V criticality of AdS black holes in a general framework, *Phys. Lett. B* **773**, 203 (2017).
- [17] B. P. Dolan, Pressure and compressibility of conformal field theories from the AdS/CFT correspondence, *Entropy* **18**, 169 (2016).
- [18] S. Cao, Y.-C. Rui, and X.-H. Ge, Thermodynamic phase structure of complex Sachdev-Ye-Kitaev model and charged black hole in deformed JT gravity, [arXiv:2103.16270](https://arxiv.org/abs/2103.16270).
- [19] A. Dehyadegari, B. R. Majhi, A. Sheykhi, and A. Montakhab, Universality class of alternative phase space and Van der Waals criticality, *Phys. Lett. B* **791**, 30 (2019).
- [20] A. Mandal, S. Samanta, and B. R. Majhi, Phase transition and critical phenomena of black holes: A general approach, *Phys. Rev. D* **94**, 064069 (2016).
- [21] A. Chamblin, R. Emparan, C. V. Johnson, and R. C. Myers, Charged AdS black holes and catastrophic holography, *Phys. Rev. D* **60**, 064018 (1999).
- [22] C. Niu, Y. Tian, and X.-N. Wu, Critical phenomena and thermodynamic geometry of Reissner-Nordström-anti-de Sitter black holes, *Phys. Rev. D* **85**, 024017 (2012).
- [23] J. Zaanen, Y. Liu, Y.-W. Sun, and K. Schalm, *Holographic Duality in Condensed Matter Physics* (Cambridge University Press, Cambridge, England, 2015).
- [24] J. Maldacena, S. H. Shenker, and D. Stanford, A bound on chaos, *J. High Energy Phys.* **08** (2016) 106.
- [25] J. Wang and M. A. Anisimov, Nature of vapor-liquid asymmetry in fluid criticality, *Phys. Rev. E* **75**, 051107 (2007).
- [26] J. W. Loram, K. A. Mirza, J. R. Cooper, and W. Y. Liang, Electronic Specific Heat of  $\text{YBa}_2\text{Cu}_3\text{O}_{6+x}$  from 1.8 to 300 K, *Phys. Rev. Lett.* **71**, 1740 (1993).
- [27] B. Michon, C. Girod, S. Badoux, J. Kačmarčík, Q. Ma, M. Dragomir, H. A. Dabkowska, B. D. Gaulin, J.-S. Zhou, S. Pyon, T. Takayama, H. Takagi, S. Verret, N. Doiron-Leyraud, C. Marcenat, L. Taillefer, and T. Klein, Thermodynamic signatures of quantum criticality in cuprate superconductors, *Nature (London)* **567**, 218 (2019).
- [28] A. Legros, S. Benhabib, W. Tabis, F. Laliberté, M. Dion, M. Lizaire, B. Vignolle, D. Vignolles, H. Raffy, Z. Z. Li *et al.*, Universal T-linear resistivity and Planckian dissipation in overdoped cuprates, *Nat. Phys.* **15**, 142 (2019).
- [29] D. Kubizňák, R. B. Mann, and M. Teo, Black hole chemistry: Thermodynamics with lambda, *Class. Quantum Gravity* **34**, 063001 (2017).
- [30] S. A. Hartnoll, C. P. Herzog, and G. T. Horowitz, Holographic superconductors, *J. High Energy Phys.* **12** (2008) 015.
- [31] U. Karahasanovic, F. Krüger, and A. G. Green, Quantum order-by-disorder driven phase reconstruction in the vicinity of ferromagnetic quantum critical points, *Phys. Rev. B* **85**, 165111 (2012).
- [32] S. W. Hawking and D. N. Page, Thermodynamics of black holes in anti-de Sitter space, *Commun. Math. Phys.* **87**, 577 (1983).
- [33] Y. Sekino and L. Susskind, Fast scramblers, *J. High Energy Phys.* **10** (2008) 065.

- [34] S. H. Shenker and D. Stanford, Black holes and the butterfly effect, *J. High Energy Phys.* **03** (2014) 067.
- [35] J. Engelsöy, T. G. Mertens, and H. Verlinde, An investigation of AdS<sub>2</sub> backreaction and holography, *J. High Energy Phys.* **07** (2016) 139.
- [36] P. Nayak, A. Shukla, R. M. Soni, S. P. Trivedi, and V. Vishal, On the dynamics of near-extremal black holes, *J. High Energy Phys.* **09** (2018) 048.
- [37] U. Moitra, S. K. Sake, S. P. Trivedi, and V. Vishal, Jackiw-Teitelboim gravity and rotating black holes, *J. High Energy Phys.* **11** (2019) 047.
- [38] U. Moitra, S. P. Trivedi, and V. Vishal, Extremal and near-extremal black holes and near-CFT<sub>1</sub>, *J. High Energy Phys.* **07** (2019) 055.
- [39] Z. Luo, Y.-Z. You, J. Li, C.-M. Jian, D. Lu, C. Xu, B. Zeng, and R. Laflamme, Quantum simulation of the non-Fermi-liquid state of Sachdev-Ye-Kitaev model, *npj Quantum Inf.* **5**, 1 (2019).
- [40] A. M. Garcia-Garcia, B. Loureiro, A. Romero-Bermúdez, and M. Tezuka, Chaotic-Integrable Transition in the Sachdev-Ye-Kitaev Model, *Phys. Rev. Lett.* **120**, 241603 (2018).
- [41] J. Kim and X. Cao, Comment on “Chaotic-Integrable Transition in the Sachdev-Ye-Kitaev Model,” *Phys. Rev. Lett.* **126**, 109101 (2021).
- [42] I. R. Klebanov, A. Milekhin, G. Tarnopolsky, and W. Zhao, Spontaneous breaking of U(1) symmetry in coupled complex SYK models, *J. High Energy Phys.* **11** (2020) 162.
- [43] S. Sahoo, E. Lantagne-Hurtubise, S. Plugge, and M. Franz, Traversable wormhole and Hawking-Page transition in coupled complex SYK models, *Phys. Rev. Res.* **2**, 043049 (2020).
- [44] V. Rosenhaus, An introduction to the SYK model, *J. Phys. A: Math. Theor.* **52**, 323001 (2019).
- [45] G. Tarnopolsky, Large  $q$  expansion in the Sachdev-Ye-Kitaev model, *Phys. Rev. D* **99**, 026010 (2019).